Two-Dimensional Simulations of Single-Frequency and Beat-Wave Laser-Plasma Heating

D. W. Forslund and J. M. Kindel
Los Alamos National Laboratory, Los Alamos, New Mexico 87545

and

W. B. Mori, C. Joshi, and J. M. Dawson
University of California, Los Angeles, California 90024
(Received 9 October 1984)

Finite-beam, two-dimensional particle simulations of single- and double-frequency laser-plasma heating are presented. In the single-frequency case, Raman backscatter and side scatter initially heat the plasma. Even in the absence of strong forward Raman scattering, strong subsequent electron heating is observed. When two collinear laser beams with $\Delta\omega = \omega_p$ are used, a coherent plasma wave heats the electrons to many megaelectronvolts. In the latter case, ion dynamics eventually disrupts the heating process.

PACS numbers: 52.65.+z, 52.25.−b, 52.50.Jm

Recently there has been a great deal of interest in underdense plasma heating by intense laser beams.[1] In order to understand the various processes occurring in such a plasma, we have carried out two-dimensional (2D) mobile ion particle simulations using finite laser beams incident onto a large-scale highly underdense plasma. Previous 1D simulations have indicated that Raman backscattering (RBS) and forward scattering (RFS) can play an important role in heating the electrons to high energies in such plasmas. An important question is whether the heating process is altered by 2D effects. Some of the 2D phenomena are Raman side scattering (RSS), self-generated magnetic fields, Weibel instabilities, whole beam self-focusing, and filamentation. In this Letter we show that these competing effects do indeed occur. Furthermore, at very high laser intensities electrons can be strongly heated even in the absence of coherent forward Raman scattering.

In order to understand the energies of electrons produced in wave-particle interactions, 2D simulations of beat heating of the plasma by two collinear lasers with frequency difference equal to the plasma frequency have been carried out. In this case a very coherent, large-amplitude plasma wave is set up at wave number $k_p = k_0 - k_1$. The time to saturation and the saturation amplitude of the plasma wave electric field is in reasonable agreement with Rosenbluth and Liu's[2] theory. This coherent plasma wave heats the electrons to many megaelectronvolts and produces maximum electron energies predicted by single-particle theory.[3]

The simulations were carried out using the particle code WAVE on a Cartesian grid in the x-y plane. The plasma is $60c/\omega_p$ long in both x and y. The laser beam has a $\cos^2 y$ transverse profile with zero amplitude at $10c/\omega_p$ and $50c/\omega_p$ in y. Other parameters are $T_i/T_e = 1$, $m_i/m_e = 1836$, and $(2kT/mc^2)^{1/2} = 0.1$. Simulations were carried out with different laser and plasma parameters to cover the parameter regime of interest in both laser fusion and the plasma beat-wave accelerator.[3] As representative of these simulations, we discuss two particular cases in this paper.

First, a single-frequency laser beam with an rms intensity $v_0/c = 0.8$ and a rise time τ of $800/\omega_p$ is injected from the left-hand boundary in the x direction into a plasma with $\omega_0/\omega_p = 5$. Here $V_0/c = eE_z/mc\omega_0$ is the quiver velocity in the laser field E_z and ω_0/ω_p is the ratio of the laser frequency to the plasma frequency. Raman backscatter/stimulated Compton scatter (SCS) is first to appear with a broad frequency spectrum peaked at frequency $\omega_0 - \omega_p$ at time $300/\omega_p$. The RBS/SCS plasma wave with $v_\phi/v_{\rm th} \sim 1.5$ does trap and heat a few electrons to a maximum energy of ~ 100 keV. An interesting feature revealed by the 2D simulations, as shown in the contour plot of Fig. 1(a) even at this early stage, is the generation of a magnetic field in such an underdense plasma. At this early time, $300 \times \omega_p^{-1}$, the magnetic field is typically $\omega_c/\omega_p \sim 0.1$ (~ 200 kG for CO_2 parameters) and has a pattern characteristic of hot-electron filamentation due to the Weibel instability,[4] as shown in the slice plot of Fig. 1(b). On the other hand, later in time when direct laser heating dominates, the magnetic field can reach $\omega_c/\omega_p \sim 0.6$ and it is indicative of a current pattern produced by a single beam of energetic electrons moving down the axis and a relatively colder return current of electrons on the outside of the directed electron beam.

The most striking difference between the 1D and 2D simulations, however, is the occurrence of RSS in the latter. RBS evolves very quickly into RSS as the plasma begins to heat up and damping for the short-wavelength plasmons increases. Initially, RSS occurs in the backward hemisphere over a broad range of angles but at later times occurs predominantly in the forward hemisphere. In Fig. 1(c) the contour plot of the

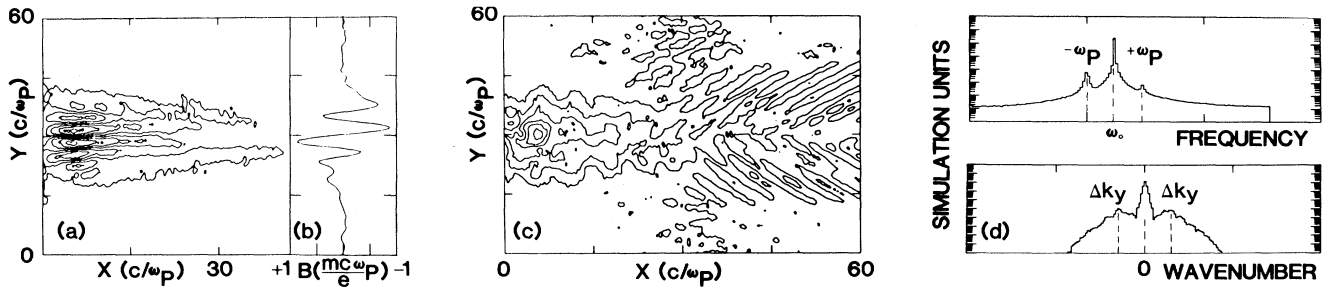

FIG. 1. (a) The contours of the self-generated magnetic field at $390/\omega_p$ by RBS. (b) The corresponding slice plot of B_z vs y. (c) The potential contour at $420/\omega_p$ showing clear evidence of RSS in the forward direction. (d) The frequency and k_y spectrum of the forward-scattered light.

plasma potential is shown at $420/\omega_p$. The most dominant side scatter mode is clearly visible at a scattering angle $\theta = 50°$. For $\omega_0 >> \omega_p$, from k matching the plasma-wave wave number is given by

$$k_p = k_0 \cos\theta \pm (k_0^2 \cos^2\theta - 2\omega_p\omega_0/c^2)^{1/2} \quad (1)$$

where + refers to backscatter and − to forward scatter. The maximum value of k_p for forward scatter (it is actually RSS in the forward direction) is $(2\omega_p\omega_0)^{1/2}/c$ and occurs for $\cos\theta = (2\omega_p/\omega_0)^{1/2}$ where θ is the angle between the laser and the plasma wave. For our case, θ should be 51°. Thus, the most dominant RSS mode observed in simulations is the largest wave-number forward-scatter mode where forward and backscatter become indistinguishable. The spectrum of the light leaving the right-hand boundary is shown in Fig. 1(d). From the upper part it is clear at this time that most of the scattered light is red-shifted (Stokes), although there is some blue-shifted (anti-Stokes) light, which is indicative of four-wave Raman. In the lower part of Fig. 1(d) the large peak in the center corresponds to the incident beam while the broad side-scattered peaks correspond to the sideband frequencies. At this time $v_0/c \sim 0.4$, and the ion density contour plot as well as the laser beam contour plot show no evidence of laser self-focusing. In Fig. 2(a) we show a 3D plot of the laser beam at $950\omega_p^{-1}$. Evidence of both whole beam self-focusing and breakup into filaments can be seen. In simulations for which ions are held fixed, self-focusing and/or filamentation occur because of relativistic effects[5] on a similar time-scale and they enhance the local laser intensity. In mobile ion simulations, relativistic effects enhance the ponderomotive self-focusing.

Interestingly, as previously noted, even without significant forward scattering energetic electrons and substantial heating are still observed. The source for the energetic electrons can be identified from the x-momentum P_x vs z-momentum P_z phase-space plot shown in Fig. 2(b) where electrons with the largest P_x also have large $\pm P_z$. This is consistent with the equations describing an electron's motion in the fields of a single intense laser,[6]

$$P_x = (-k^2 + m^2c^2 + P_z^2)/2k; \quad P_z = f + eA_z/c \quad (2)$$

where A_z is the vector potential and f and k are the constants of motion. These equations by themselves do not give rise to particle heating. However, the presence of additional waves can lead to stochastic motion. In particular, it has been shown both analytically and numerically[6] that the inclusion of a second, counter-propagating, electromagnetic wave leads to stochastic behavior if threshold conditions are exceeded. We have observed such heating both with and without a density jump exceeding n_c that reflects the incoming light, although with reflection the heating

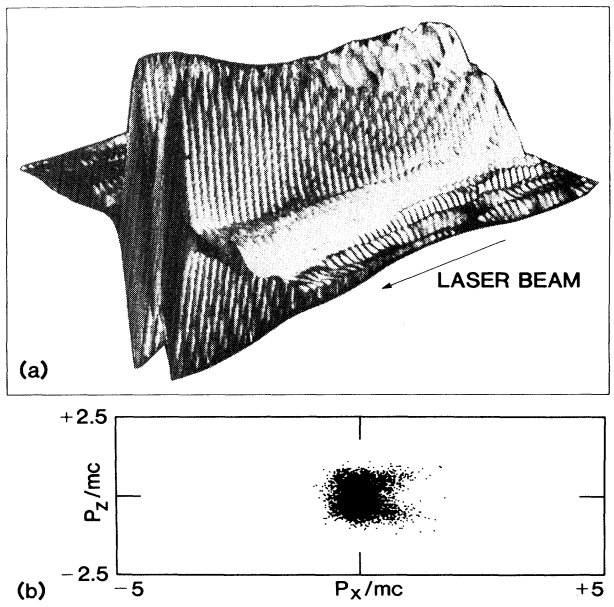

FIG. 2. (a) The 3D plot of the electric field of the laser at $950/\omega_p$ showing laser beam self-focusing. (b) Electron P_z vs P_x phase space at $480/\omega_p$.

occurs earlier. Energies as high as 5–7 MeV have ultimately been observed leaving the right-hand boundary.

In order to quantitatively understand the energies of electrons produced by particle trapping in a plasma wave, we have carried out 2D simulations of beat excitation in underdense plasmas.[3] Two collinear laser beams of equal amplitude and a total rms $v_0/c = 0.8$, $\tau = 800/\omega_p$, and frequencies $\omega_0 = 5\omega_p$ and $\omega_1 = 4\omega_p$ are injected in a homogeneous plasma. Before showing the details of the simulations, we indicate fluid and single-particle theory results which are confirmed in our 1D and 2D simulations.[3] First, we find that for lasers with a finite rise time the time for the plasma wave to reach saturation can be described by a straightforward modification of the fluid treatment of Rosenbluth and Liu.[2] The time to saturation can be found by solving the following equation for time t:

$$\frac{\omega_p}{4}\int_0^t [\alpha_1(t')\alpha_2(t')]dt' = [(\tfrac{16}{3})\alpha_1(t)\alpha_2(t)]^{1/3} \quad (3)$$

where $\alpha_1(t) = v_0/c$. The left-hand side is the plasma wave amplitude and the right-hand side is the instantaneous relativistic saturation amplitude. Assuming a linear rise time τ for the two lasers, the time to saturation t_s is

$$\omega_p t_s = 3.68(\omega_p\tau)^{4/7}(\alpha_1\alpha_2)^{-2/7} \quad (4)$$

where $\alpha_1(t) = \alpha_1 t/\tau$. The saturation amplitude $\epsilon = (eE_x/m_e c\omega_p)$ can be obtained by substituting t_s for t in the left-hand side of Eq. (3) provided that $t_s < \tau$. Here E_x is the longitudinal electric field of the plasma wave. Second, single-particle theory[3] shows that an electron trapped in a plasma wave of amplitude ϵ and moving at v_ϕ can acquire a maximum amount of energy $4\epsilon\gamma_\phi^2 mc^2$ where for a plasma wave excited by beat-wave excitation $\gamma_\phi = (1 - v_\phi^2/c^2)^{-1/2} \sim \omega_0/\omega_p$.

Figure 3(a) is a 3D plot of the scalar potential of the plasma wave at $330\omega_p^{-1}$. In contrast to single-frequency simulations, a very coherent plasma wave, $k_p = k_0 - k_1$, is now set up through optical mixing. According to Eq. (3), when actual rise times are used, the plasma wave amplitude should be $\epsilon = 0.55$ at $t = 330/\omega_p$. In simulations we observe $\epsilon = 0.5$ in good agreement with the fluid theory. Although it is not presented here, the longitudinal electric field begins to decay after reaching saturation in both our 1D and 2D simulations, as predicted by the fluid theory.[3]

The evolution of the electron phase space is complicated because the plasma wave builds up to saturation and decays several times before trapped particle damping and ion dynamics disrupt the acceleration process. During the first buildup phase, although the longitudinal field is extremely large in absolute terms because it

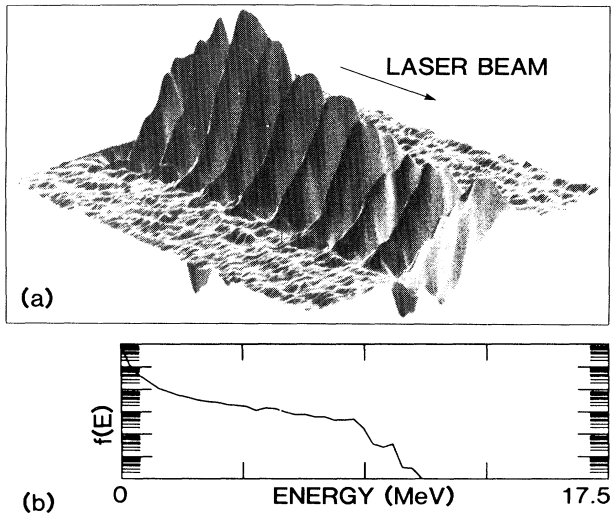

FIG. 3. (a) The 3D plot of the plasma wave electric field at $330/\omega_p$ excited by optical mixing. The electric field reaches a maximum value $\epsilon = 0.5$ at the left-hand boundary. (b) The electron distribution function at $450/\omega_p$ showing electron heating to 11 MeV.

is only about half the wave-breaking limit, very few electrons can be trapped from the background 2.5 keV plasma. By the time the plasma wave has built up for the second time, the background plasma is already heated up because of RBS and direct laser heating and a significant number of electrons can therefore be trapped and accelerated. In contrast to the single-frequency simulation, electrons with large P_x have small P_z. It is therefore simple to determine whether acceleration is resulting directly from longitudinal or transverse waves. In simulations a quantitative measure of the electron heating is obtained from the electrons striking the right-hand boundary. The accelerated particles at $450/\omega_p$ have a truncated 1D "Maxwellian" distribution [Fig. 3(b)] with a temperature $T_H \sim 5.5$ MeV and a cutoff energy at 11 MeV. In other simulations[3] in which shorter rise times were employed, the maximum energies were in very good agreement with the single-particle theory. For longer rise times the plasma wave loses coherence by scattering off ion flucutations at wavelengths peaking around one-half of the plasma wavelength.

The plasma wave begins to lose coherence and eventually disrupts as competing phenomena come into play. On an ω_p^{-1} time scale, RBS, RSS, RFS, and the laser itself heat up the plasma and produce bandwidth, while relativistic self-focusing enhances the on-axis laser intensity. On somewhat longer time scales, parametric decay destroys the plasma wave and finally ponderomotive self-focusing destroys the resonance condition and eventually terminates the heating pro-

cess.

At times when the plasma wave is very effectively accelerating electrons, the overall absorption can be as high as 15 percent over the computational box. At later times, when competing mechanisms reduce the plasma wave coherence and acceleration is relatively inefficient, the absorption drops to a few percent.

We wish to thank Dr. F. F. Chen, Dr. T. C. Katsouleas, Dr. C. E. Clayton, Dr. D. Bach, Dr. F. Felber, Dr. P. Goldstone, Dr. S. Singer, and Dr. R. Bingham for many stimulating discussions. This work was supported by the U. S. Department of Energy and by the National Science Foundation.

[1]D. W. Phillion *et al.*, Phys. Rev. Lett. **49**, 1405 (1982); C. Joshi *et al.*, Phys. Rev. Lett. **47**, 1285 (1981); K. Estabrook, W. L. Kruer, and B. F. Lasinski, Phys. Rev. Lett. **45**, 1399 (1980); D. W. Forslund, J. M. Kindel, and E. Lindman, Phys. Rev. Lett. **30**, 739 (1973).

[2]M. N. Rosenbluth and C. S. Liu, Phys. Rev. Lett. **29**, 701 (1982).

[3]C. Joshi *et al.*, Nature **311**, 525 (1984); T. Tajima and J. M. Dawson, Phys. Rev. Lett. **43**, 267 (1979); B. I. Cohen, A. N. Kaufman, and K. M. Watson, Phys. Rev. Lett. **29**, 581 (1972); W. B. Mori, Masters thesis, UCLA, 1984 (unpublished).

[4]R. L. Morse and C. W. Neilson, Phys. Fluids **14**, 830 (1971).

[5]C. E. Max, J. Arons, and A. B. Langdon, Phys. Rev. Lett. **33**, 209 (1974).

[6]L. D. Landau and E. M. Lifshitz, *Classical Theory of Fields* (Addison-Wesley, Reading, Mass., 1971), 3rd ed.; J. T. Mendonca, Phys. Rev. A **28**, 3592 (1983).

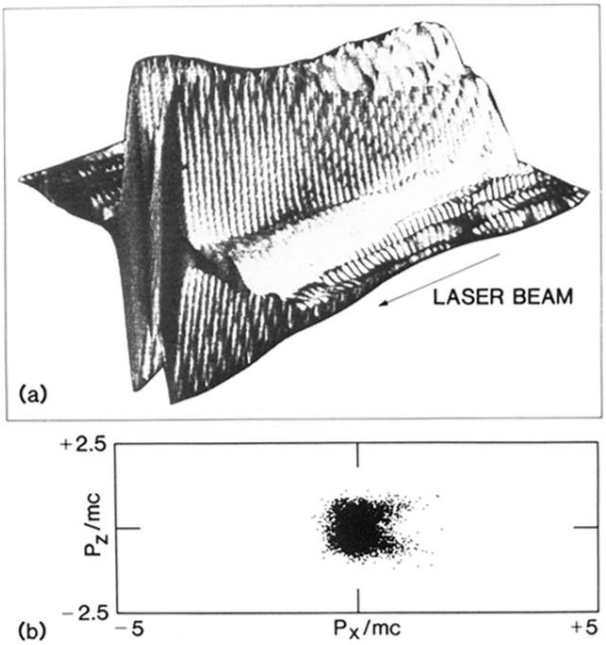

FIG. 2. (a) The 3D plot of the electric field of the laser at $950/\omega_p$ showing laser beam self-focusing. (b) Electron P_z vs P_x phase space at $480/\omega_p$.

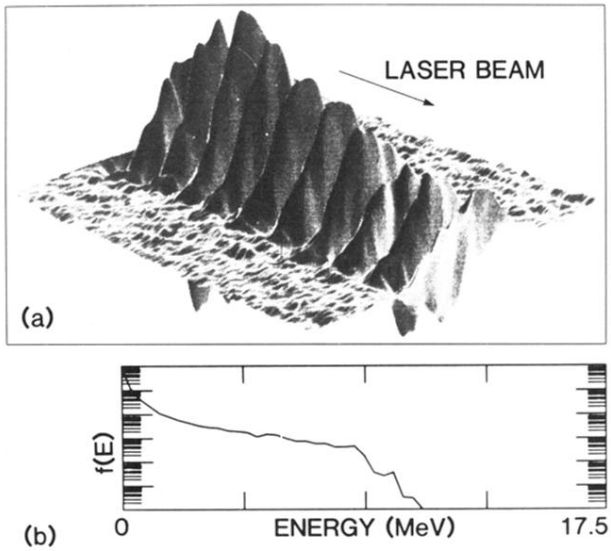

FIG. 3. (a) The 3D plot of the plasma wave electric field at $330/\omega_p$ excited by optical mixing. The electric field reaches a maximum value $\epsilon = 0.5$ at the left-hand boundary. (b) The electron distribution function at $450/\omega_p$ showing electron heating to 11 MeV.